

### §36. Improving the Hopfield Neural Network for Bolometer Tomography of LHD Plasma

Iwama, N., Ichikawa, N. (School of Informatics, Daido Inst. of Tech.),

Hosoda, Y. (Dept. of Information Science, Fukui Univ.),

Liu, Y., Tamura, N., Peterson, B.J.,

Kostyukov, A. Yu. (St. Petersburg Tech. Univ.)

The Hopfield neural network can be a tool of solving the optimization problem of Tikhonov-Phillips type with a modification of using the nonlinear activation function of sigmoid, and is applicable to plasma image reconstruction from sparse data [1]. For an  $M$ -detector imaging system of linear equation  $H\mathbf{f}=\mathbf{g}$ , the neural net is composed by giving the interconnecting weight matrix  $W=2(H^TH+M\gamma C^TC)$  and the bias vector  $\boldsymbol{\theta}=(2/M)H^T\mathbf{g}$ . Involving the Laplacian operator  $C$  in the penalty function and appropriating the regularization parameter  $\gamma$  might give a possibility of smoothing the plasma profiles as well as the Phillips method and also keeping the image values positive like the maximum entropy method (MEM).

The two fan-beam camera system with AXUVD silicon photodiodes ( $M=40$ ) that was mounted in the semi-tangential cross section using 3.5-U and 4-O ports of LHD now provides projection data well calibrated by taking into account the sensitivity difference of factor  $\sim 2$  between two cameras [2, 3]. The corrected data have been useful to reconfirm the satisfactory behavior of the neural net, that is, the monotonic decrease of the energy function and the resulting reasonable profile of emissivity, the smoothness of which has been well changed with the value of  $\gamma$  as expected. After this reconfirmation, study has been devoted to faster computing.

Firstly, with regard to the sparseness of the matrices  $H$  and  $W$ , the renovation of the neural net according to its dynamical equation can be accelerated by omitting the zero matrix elements. In fact, by computer coding with the compressed column/row storage formats (CCS/CRS formats), the computing time for one data vector  $\mathbf{g}$  has been decreased nearly by the factor of 17.4% that was the number ratio of nonzero elements in the  $K \times K$  matrix  $W$  ( $K=1024$ ). Secondly, acceleration has been obtained by changing the activation function. To avoid the saturation of sigmoid function value, one has to adopt a reductive scaling of  $\mathbf{g}$ , and resultantly one meets a slow renovation due to the low gradient of the function in negative inner-voltage region. With this regard, we take the "skimmer" function [4]

$$f_i(u_i)=u_i+\ln[1+\exp(-u_i)] \quad (i=1, 2, \dots, K),$$

which is a monotonically increasing function with  $df_i(u_i)/du_i = [1+\exp(-u_i)]^{-1}$  (i.e. the sigmoid function). When the scaling factor  $\rho$  of  $\mathbf{g}$  is increased so as to use the almost linear region of  $f_i(u_i) \propto u_i$  ( $u_i > 0$ ), we get an effective acceleration. The result of a test shown in Fig. 1 (Shot No. 31721,  $t=2$ [s]) indicates that the number of iterations of

updating the whole system of neural net to get a convergence of the energy function  $E$  can be decreased even ten-fold by replacing the sigmoid function.

Fig. 2 shows an example of the reconstructed plasma image  $\hat{\mathbf{f}}$ , which indicates the emission in the inside of a triangular border of magnetic surface and an additional emission caused by a gas puffing from the bottom. As the iteration went with a resulting approach of the projection estimate  $H\hat{\mathbf{f}}$  to data  $\mathbf{g}$ , the  $\hat{\mathbf{f}}$  gradually acquired the plasma profile, but artifacts began to grow outside the fields of vision of the two cameras. When these artifacts were diminished by giving large negative biases to the neurons in this outside region, the fitting of  $H\hat{\mathbf{f}}$  to  $\mathbf{g}$  became worse. This behavior of  $\hat{\mathbf{f}}$  might suggest a necessity of adopting the third camera for more reliable imaging.

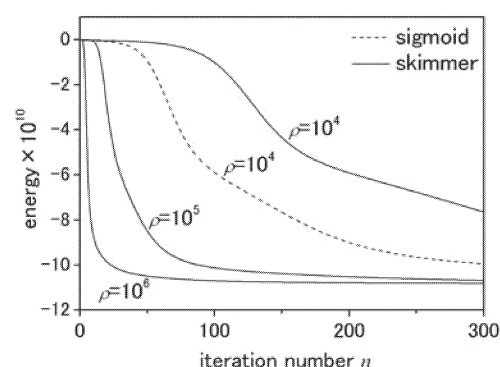


Fig. 1. Histories of the energy function of neural net with various values of  $\rho$ ;  $\gamma=1.0 \times 10^{-4}$ ,  $\Delta t=1.0$ .

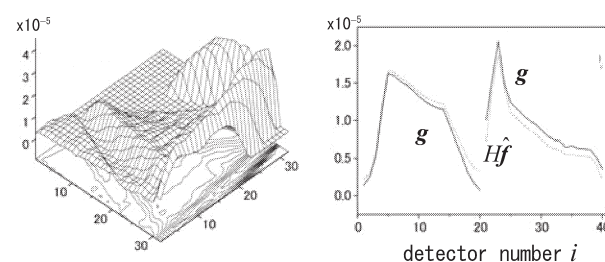


Fig. 2. Left: plasma image  $\hat{\mathbf{f}}$  reconstructed by the skimmer function ( $\rho=10^6$ ,  $n=100$ ,  $\gamma=1.0 \times 10^{-4}$ ,  $\Delta t=1.0$ ) at  $32 \times 32$  pixels. Right: its projection  $H\hat{\mathbf{f}}$  (dotted lines) and the detector outputs  $g_i$  (solid lines) of the vertical and the horizontal cameras for  $i=1 \sim 20$ ,  $21 \sim 40$ .

#### References

- 1) Iwama, N., Hosoda, Y. and Peterson, B.J., Ann. Rep. NIFS (2004-2005) 160.
- 2) Liu, Y., Tamura, N., Peterson, B.J. and Iwama, N.: Ann. Rep. NIFS (2005-2006) 59.
- 3) Liu, Y., Tamura, N., Peterson, B.J. et al.: Rev. Sci. Instrum. 77 (2006) 10F501.
- 4) Ma, X.F., Fukuhara, M., and Takeda, T.: Nucl. Instrum. Methods Phys. Res. A 449 (2000) 366.